Orbital: The Electronic Journal of Chemistry
journal homepage: www.orbital.ufms.br
e-ISSN 1984-6428

| Vol 11 | | No. 2 | | Special Issue April 2019 |

FULL PAPER

Theoretical Study of the Structural Properties of the Lead Titanate Doped with Strontium

Weber Duarte Mesquita[a], Maria Rita de Cássia Santos[b], José Waldo Martínez Espinosa[c], Sérgio Henrique Bezerra de Sousa Leal[d], Elson Longo[e], Maria Fernanda do Carmo Gurgel[a-b*]

[a]Universidade Federal de Goiás - Regional Catalão, Programa de Pós-Graduação em Ciências Exatas e Tecnológicas - PPGCET, Av. Dr. Lamartine Pinto de Avelar, 1120, CEP: 75704-020, Catalão - GO, Brazil.
[b]Universidade Federal de Goiás - Regional Catalão, Unidade Acadêmica Especial de Química, Av. Dr. Lamartine Pinto de Avelar, 1120,CEP: 75704-020, Catalão - GO, Brazil.
[c]Universidade Federal de Goiás - Regional Catalão, Faculdade de Engenharia - FENG - Engenharia de Produção. Av. Dr. Lamartine Pinto de Avelar, 1120, CEP 75704-020, Catalão - GO, Brazil.
[d]Universidade Federal do ABC, Centro de Ciências Naturais e Humanas. Rua Santa Adélia, 166, Bloco A, Torre 3, CEP 09210-170, Santo André-SP, Brazil.
[e]Universidade Federal de São Carlos (UFSCar), Departamento de Química, São Carlos, SP, Jardim Guanabara, CEP 13565-905, São Carlos- SP, Brazil.

Article history: Received: 10 Ocrtober 2018; revised: 04 December 2018; accepted: 07 February 2019. Available online: 11 April 2019. DOI: http://dx.doi.org/10.17807/orbital.v11i2.1342

Abstract:

Combined experimental and theoretical approach to investigate the structural and electronic properties to Sr-doping lead titanate (PT:Sr) was carry out. It is well-known at room temperature PT crystallizes in tetragonal distorted perovskite structure with space group symmetry P4mm. At higher temperature (T > 490 °C), this compound presents a tetragonal-cubic phase transition and, due to its high tetragonality (c/a), the PT ceramics can develop cracks during the cooling process. The Sr-doping reduce this lattice anisotropy, and the doped ceramics become denser than the pure ones.The ceramic materials lead titanate (PT), lead strontium titanate (PST) and strontium titanate (ST) were synthetized by Polymeric Precursor Method. The crystal structure systems are taken from Rietveld refinement. These materials were characterized by theoretical X-ray diffraction data, total state densities (DOS), Gap values and charge maps. The gap values obtained were 3.60 eV, 3.20 eV and 3.70 eV for PT, PST and ST, respectively. The c/a ratio was investigated with different strontium concentration in the PT structure, showing that the tetragonality decreased from tetragonal to pseudo-cubic. Therefore, decreases tetragonality (c/a) and improves the physicochemical properties of the material. The presence of the atom in the PT matrix promotes an electronic stability in the strucutre of the PST inducing an improvement in the proportions of the material. In addition, ferroelectric properties can be adjusted by altering the Pb/Sr molar ratio. This behavior was associated to a lattice contraction effect caused by the diferent ionic radii between Pb and Sr. In this context, the present study characterizes the effects of Sr-doping upon structural and electronic properties of lead titanate matrix (PT). A periodic quantum-mechanical method based on DFT theory at B3LYP level has been used. These theoretical results are in agreement with the experimental.

Keywords: Band; crystalline; DFT; gap; PST

1. Introduction

Perovskite compounds with chemistry formula ABO_3, where A = Ba, Sr, Ca or Pb, and B = Ti, Zr or Mo. These materials may be cubic, tetragonal or orthorhombic and can be used in ultrasonic transducers for medical and sonar applications, infrared sensors and non-volatile, random-access ferroelectric memory (FRAM) [1-9]. Anisotropy occurs in the tetragonal phase and sintering induces a transition from the cubic-tetragonal phase, resulting in structural stress and a porous, fragile material with weak polarization [2, 3, 5, 6, 10]. PT has a tetragonal crystalline structure

*Corresponding author. E-mail: mfcgurgel@outlook.com

(space group *P4mm*) at room temperature. However, upon reaching the Curie temperature (T_c = 490 °C), c/a decreases by approximately 6%, resulting in a phase transition to a cubic system (space group *Pm3m*) in which a transition from the ferroelectric phase to the paraelectric phase is evidenced. Lead titanate (PT) is characterized by a phase transition as temperatures change within a given interval and the presence of ions within its matrix [2, 6, 11-14]. The partial substitution of rare earth elements (RE) and other ions, produces ceramics that are free from cracks and that have denser structures with reduced T_c and tetragonality (c/a) [11, 15, 16].

Gurgel et al. used quantum mechanical calculations to demonstrate the influence of Sm on the PT matrix, showing the presence of the Jahn Teller effect, caused by the structural readjustment of atoms. A quantum mechanical study showed that the presence of Er atoms in the PT structure favors a transition from tetragonal to cubic that reduces the tetragonality (c/a) generated by a small disturbance in the energy levels of the atomic orbitals within the structure [1, 17]. Substituting Pb^{2+} with Ca^{2+}, Sr^{2+} or Ba^{2+} significantly reduces the Curie temperature (T_c) and decreases the tetragonality at ambient temperatures that is caused by differences in the ionic radii of the substituents. Materials of type

$Pb_{1-x}Ca_xTiO_3$ (PCT), $Pb_{1-x}Sr_xTiO_3$ (PST) and $Pb_{1-x}Ba_xTiO_3$ (PBT), obtained by incorporating Ca^{2+}, Sr^{2+} and Ba^{2+} ions into the PT matrix, improve ferroelectric properties and produce high-quality, chemically-homogeneous PST compounds [6, 12, 15, 18-23].

According to Leal et al. [19], the process of obtaining PST with the presence of Sr in the PT matrix results in a stoichiometric compound that, in addition to allowing control over properties also minimizes problems related to the sintering of the PT base materials. In addition, ferroelectric properties can be adjusted by altering the Pb/Sr ratio. PST has differentiated physicochemical properties. The presence of Sr in the PT matrix induces localized structural micro-development in the paraelectric phase and increases strontium concentration in the PT matrix, which in turn decreases tetragonal distortion in the octahedron (TiO_6) caused by network contraction that results from the difference between the ionic radius of Pb and Sr [18-21]. In the current study, we performed theoretical calculations (VESTA [24], CRYSTAL [25, 26] and XCrysden [27] programs) to analyze the structural and electronic properties of PT, PST and ST and investigate the influence of Sr on the PT matrix. Our results were interpreted in terms of theoretical XRD, DOS, gap, band structure, charge mapping and electronic density. Periodic models (1x1x2) were simulated using the Rietveld refinement results reported by Leal et al. [19]

2. Results and Discussion

The Rietveld Refinement results for PT, PST and ST, according to Leal et al. [19], supported the construction of the three (1x1x2) models, respectively. Figure 1(a-c) shows representations of the periodic superposition (1x1x2) models for PT, PST and ST, respectively.

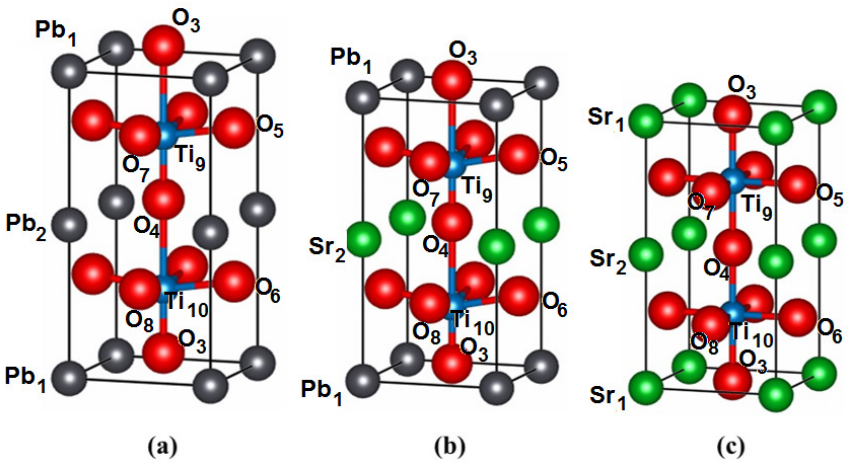

Figure 1. Representation of the (1x1x2) supercell models (a) PT, (b) PST and (c) ST.

Each model has two titanium atoms that act as network formers and are located at the center of each cluster [Ti_9-O_6] - [Ti_{10}-O_6] and sixfold oxygen Ti_9 and Ti_{10} coordination O_1, O_2, O_3, O_4, O_5, O_7 and O_1, O_2, O_3, O_4, O_6, O_8, respectively. The lead, strontium-strontium and strontium atoms are located at the vertices of the PT, PST and ST compounds, respectively.

Figure 2(a-c) illustrates the theoretical diffractograms of PT, PST and ST obtained using the VESTA program [24]. X-ray diffraction analysis was performed to correlate the theoretical computational results with the experimental results reported by Leal et al. [19]. Figure 2a and c illustrate the theoretical diffractograms of PT and ST, respectively, and show the characteristic peaks of the crystalline structures of these materials. These agree with the peak indices from the JCPDS-ICDD cards N °06-0452 and 035-0734 for PT and ST, respectively. PT has a perovskite structure of the tetragonal type, space group P4/mmm (crystallographic report 06-0452), while ST has a cubic structure with a Pm-3m space group (crystallographic report 035-0734).

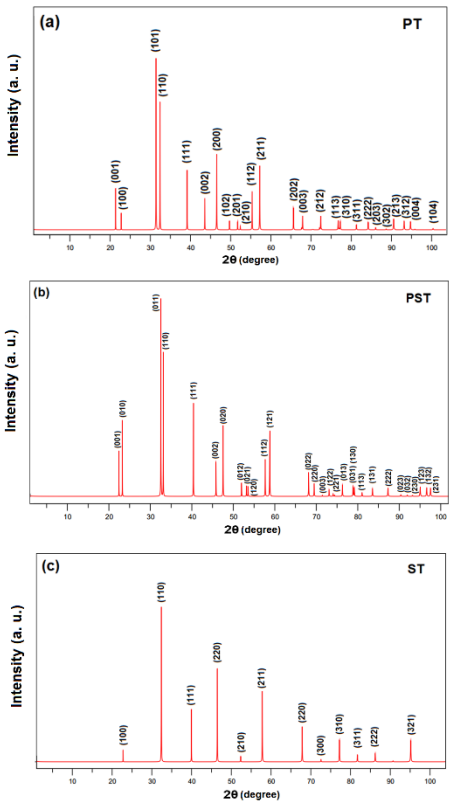

Figure 2. Theoretical X-ray diffraction of (a) PT, (b) PST and (c) ST using VESTA program.

Figure 2 (a-c) depicts the theoretical XRD of PT, PST and ST, respectively. Figure 2 (a-b) shows that the crystal structure of PT is distorted tetragonal while ST is cubic. The theoretical diffractograms of the PST structure (Figure 2b) shows a narrowing of the peaks (001) and (100) that correspond to the next 2θ values of 21 and 23 degrees, suggesting that the addition of Sr in PT causes intermediate phase distortion from tetragonal to pseudo-cubic.

The theoretical XRD of PT in Figure 2a illustrates the tetragonal phase (P4/mmm) indexed with crystallographic report 06-0452. The crystallinity of the material is confirmed by the presence of peaks (001), (100), (101), (110), (111), (002), (200), (102), (201), (210), (210), (112), (211) reported by various authors [28-33]. Figure 2b shows the theoretical XRD of PST with peaks (001), (110), (111), (002), (112), (121) that agree with the literature [19, 34-36]. The theoretical XRD of PST demonstrates that the material is in the pseudo-cubic phase, where increasing levels of Sr atoms induce structural deformation, characterized by conversion from peaks of the tetragonal (PT) to those of the cubic structure (ST). Figure 2c shows that the theoretical XRD of ST represents the cubic phase (Pm3m) indexed with crystallographic report 035-0734. The crystallinity of the material is confirmed by the presence of peaks (100), (110), (111), (210), (211), (220), (300) and (310) that have been reported by various authors [19, 37-41].

Table 1. Crystalline structure, gap values and tetragonaility of PT, PST and ST.

Compound	Structure	Gap (eV)	Tetragonality (c/a)
PT	Tetragonal	3.60	1.06
PST	Pseudo-cubic	3.20	1.01
ST	Cubic	3.70	1.00

The c/a values in Table 1 show that the PT, PST and ST compounds have tetragonal, pseudo-cubic and cubic crystalline structures, respectively. These differences in structure are due to the influence of the Sr atom in the PT matrix [2]. The presence of strontium induces structural deformation in the PT matrix, resulting in PST. Therefore, the c/a values in Table 1 tend towards

the cubic structure. This phase transition is caused by a change in the lattice parameters (c and a) of the perovskite structure. The addition of Sr in the PT matrix gradually increases the a-axis and decreases the c-axis resulting in a lower unit-cell volume [19-24]. The PT gap value in Table 1 agrees with those reported in the literature [1]. Table 1 also shows that the PT and ST gap values are greater than that of PST, suggesting that Sr in the PT matrix induced structural and electronic changes that improved physicochemical properties [1, 11-15, 17]

The density of states in Figure 3(a-c) was used to analyze hybridization between the atomic orbitals of the O and Ti of PT, PST and ST.

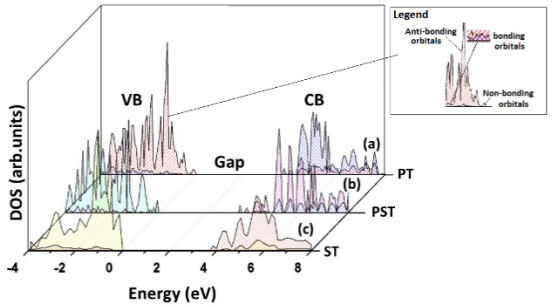

Figure 3. Total DOS representing hybridization between the oxygen and titanium atoms of (a) PT, (b) PST and (c) ST.

Figure 3(a-c) shows the total density of states (DOS) with the electronic contributions of the atomic orbitals from the Ti and O atoms in PT, PST and ST with a gap value of 3.60 eV, 3.20 eV, 3.70 eV, respectively. In these figures, the superposition of the total density of states (DOS) of the Ti and O atoms illustrates the regions where hybridization occurs between the Ti and O atoms. Therefore, the CB (conduction band) and VB (valence band) regions show the bonding orbitals, the non-bonding orbitals and the anti-bonding orbitals. Hybridization regions are where intercession occurs between the electronic contributions of the atomic orbitals of the Ti and O atoms. The regions of the VB and the CB in which the hybridizations take place are designated as binding orbitals. This suggests that Ti-O is linked by chemical bonds of a covalent character. The total projections of the density of states of the oxygen atoms show that the total electronic contributions from the atomic orbitals (p_x, p_y, p_z) are predominantly located in the VB region. The electronic contributions from the atomic orbitals (d_{xy}, d_{xz}, d_{yz}, $d_{x^2-y^2}$, d_{z^2}) of the Ti atoms occur in the CB region. The VB region of PT (Figure 3a) illustrates that electronic contributions occur between 3.60 eV to 8.20 eV and from 0 to -4.72 eV. Figure 3b shows that the electronic contributions of PST are between 3.20 eV and 9.17 eV for CB and between 0 and -5.03 eV for VB. For ST, the CB region is located between 3.70 eV and 10.49 eV while the VB is between 0 and -4.02 eV (Figure 3c).

Figure 4(a-c) illustrates the charge mapping in the (1 1 0) plane for PT, PST and ST, respectively. The plotted diagonal plane corresponds to the Pb_1, Ti_9, Ti_{10}, O_3 and O_4 atoms and was used to analyze the charge maps for these models. The models are represented by contour lines in the plotted plane.

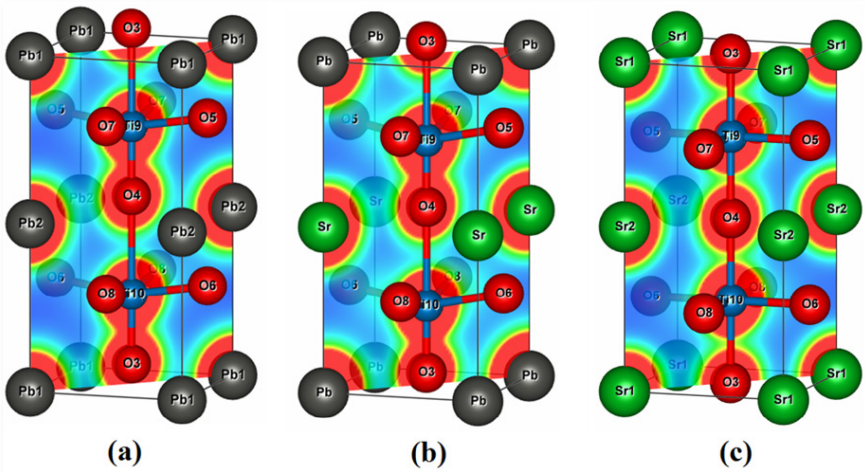

Figure 4. Representation of the charge mapping in the (1 1 0) plane for (a) PT, (b) PST and (c) ST.

Figure 4(a-c) shows that Pb_1-O_3-Ti_9-O_4-Ti_{10}-O_3-Pb_1 atoms are present in the diagonal plane for PT, PST and ST, respectively. The load map for PT in Figure 4a illustrates that the contour lines are homogeneous and that the structure is distorted-tetragonal, given that the Ti and O atoms in the z axis are below and above the xy plane, respectively. The homogeneous contour lines of the PST structure are illustrated in Figure 4b and show a small structural deformation between the atoms in the PST structure that induces a pseudo-cubic structure. The ST charge map in Figure 4c shows that a change occurred in the contour lines of the atoms in this structure. The absence of Pb caused the structure to shift from pseudo-cubic to cubic. This fact, and the homogeneous and symmetrical behavior of the contour lines are characteristic of the cubic structure [1,2]

3. Material and Methods

The ceramic materials lead titanate doped with strontium were obtained using the Polymer Precursor Method (MPP) from Leal et al. [19] who reported Rietveld refinement data for PT, ST and PST. The Rietveld refinement data were then used for calculations and to construct theoretical models (1x1x2) for these materials. The VESTA [24] and CRYSTAL [26] and XCrySDen [27] packages were used for computational simulations.

All computational simulations were used with the Density Functional Theory (DFT) proposed by Lee, Yang and Parr [42] combined with the gradient-corrected correlation functional (B3LYP), in conjunction with Becke's three parameter hybrid nonlocal exchange functional [43] using the CRYSTAL software [26]. The CRYSTAL package is a periodic ab initio quantum-mechanical calculation which was used to study the BSTs structural and electronic properties. The basic set described: Durand-31G* for Pb [44], 6-411(d31)G for Ti [45,46], 6-31d1 for O [47] and 976-41(d51)G for Sr [48]. The functional B3LYP was chosen due to its potential for reproduce with accuracy the electronic properties of semiconductor materials [49], and the lattice parameters in our case gave the best agreement if compared with experimental results [50].

4. Conclusions

Theoretical and experimental approach show that PT, PST and ST structures are distorted tetragonal, pseudo-cubic and cubic, respectively. Our theoretical XRDs agree with the XRD results reported in the literature. The theoretical total DOS of the Ti and O atoms, charge mapping results and c/a show that structural readjustment occurs among atoms and leads to electronic stability in PT, PST and ST. While this structural change is small, it does produce changes in gap values. Our study also revealed that pure PT (c/a = 1.06) is porous and fragile due to structural tensions that cause micro and macro-cracks. However, the presence of Sr atoms in the PT matrix causes structural readjustment of the atoms and forms PST. This in turn decreases tetragonality (c/a) and improves the physicochemical properties of the material.

Acknowledgments

CAPES, FAPEG, CNPq, FAPESP, UFG-DQ-RC and CDMF for their support and partnership and J. A. Varela in memory.

References and Notes

[1] Gurgel, M. F. C.; Paris, E C.; Espinosa, J. W. M.; Paiva-Santos, C. O.; Leite, E. R.; Souza, A. G.; Varela, J. A.; Longo, E. *J. Mol. Struct.: THEOCHEM* **2007**, *813*, 33. [Crossref]

[2] Ahmad, A.; Bedard, P.; Wheat, T. A.; Kuriakose, A. K.; McDonald, A. G. *J. Solid State Chem.* **1991**, *93*, 220. [Crossref]

[3] Iljinas, A.; Stankus, V.; Čyvienė, J.; Abakevičienė, B. *Vacuum* **2015**, *122*, 310. [Crossref]

[4] Giridharan, N. V.; Jayavel, R. *Mater. Lett.* **2002**, *52*, 57. [Crossref]

[5] Ohno, T.; Suzuki, H.; Fu, D.; Takahashi, M.; Ota, T.; Ishikawa, K. *Ceram. Int.* **2004**, *30*, 1487. [Crossref]

[6] Shirane, G.; Hoshino, S.; Suzuki, K. *Phys. Rev.* **1950**, *80*, 1105. [Crossref]

[7] Patel, N. D.; Mangrola, M. H.; Soni, K.G.; Joshi, V. G. *Mater. Today: Proc.* **2017**, *4*, 3842. [Crossref]

[8] Sangawar, S. R.; Praveenkumar, B.; Divya, P.; Kumar, H. H. *Mater. Today: Proc.* **2015**, *2*, 2789. [Crossref]

[9] Murtaza, T.; Ali, J.; Khan, M. S.; Asokan, K. *J. Mater. Sci.: Mater. Electron.* **2018**, *29*, 2110. [Crossref]

[10] Bhatti, H. S.; Hussain, S. T.; Khan, F. A.; Hussain, S. *Appl. Surf. Sci.* **2016**, *367*, 291. [Crossref]

[11] Peláiz-Barranco, A.; Guerra, J. D. S.; Calderón-Piñar, F.; Aragó, C.; García-Zaldívar, O.; López-Noda, R.; Gonzalo, J. A.; Eiras, J. A. *J. Mater. Sci.* **2009**, *44*, 204.

[Crossref]

[12] Bretos, I.; Ricote, J.; Jiménez, R.; Mendiola, J.; Jiménez Riobóo, R. J.; Calzada, M. L. *J. Eur. Ceram. Soc.* **2005**, *25*, 2325. [Crossref]

[13] Erdem, E.; Kiraz, K.; Somer, M.; Eichel, R.-A. *J. Eur. Ceram. Soc.* **2010**, *30*, 289. [Crossref]

[14] Zhou, W.; Deng, H.; Yu, L.; Yang, P.; Chu, J. *J. Appl. Phys.* **2015**, *117*, 194102. [Crossref]

[15] Pontes, F. M.; Santos, L. S.; Rissato, S. R.; Pontes, D. S. L.; Longo, E.; Leite, E. R.; Claro Neto, S.; Chiquito, A. J.; Pizani, P. S. *J. Phys. Chem. Solids* **2008**, *69*, 2796. [Crossref]

[16] Gong, S.; Ren, Z.; Jiang, S.; Li, M.; Li, X.; Wei, X.; Xu, G.; Shen, G.; Han, G. *J. Phys. Chem. C* **2014**, *118*, 5486. [Crossref]

[17] Paris, E. C.; Gurgel, M. F. C.; Boschi, T. M.; Joya, M. R.; Pizani, P. S.; Souza, A. G.; Leite, E. R.; Varela, J. A.; Longo, E. *J. Alloys Compd.* **2008**, *462*, 157. [Crossref]

[18] Leal, S. H.; Escote, M.T.; Pontes, F. M.; Leite, E. R.; Joya, M. R.; Pizani, P. S.; Longo, E.; Varela, J. A. *J. Alloys Compd.* **2009**, *475*, 940. [Crossref]

[19] Leal, S. H.; Sczancoski, J. C.; Cavalcante, L. S.; Escote, M. T.; Matos, J. M. E.; Santos, M. R. M. C.; Pontes, F. M.; Longo, E.; Varela, J. A. *J. Sol-Gel Sci. Technol.* **2010**, *53*, 21. [Crossref]

[20] Pontes, F. M.; Leal, S. H.; Leite, E. R.; Longo, E.; Pizani, P. S.; Chiquito, A. J.; Varela, J. A. *J. Appl. Phys.* **2004**, *96*, 1192. [Crossref]

[21] Pontes, F.; Leal, S.; Pizani, P.; Santos, M.; Leite, E.; Longo, E.; Lanciotti, F.; Boschi, T.; Varela, J. A. *J. Mater. Res.* **2003**, *18*, 659.

[22] Nagarbawadi, M. A.; Jangade, P. S.; Bagwan, S. T. *IOSR J. Appl. Phys.* **2014**, *6*, 15. [Crossref]

[23] Huang, X. -X.; Zhang, T. -F.; Tang, X. -G.; Jiang, Y. -P.; Liu, Q. -X.; Feng, Z. -Y.; Zhou, Q. -F. *Sci. Rep.* **2016**, *6*, 31960. [Crossref]

[24] Momma, K.; Izumi, F. *J. Appl. Crystallogr.* **2011**, *44*, 1272. [Crossref]

[25] Dovesi, R.; Orlando, R.; Civalleri, B.; Roetti, C.; Saunders Victor, R.; Zicovich-Wilson Claudio, M. *Zeitschrift für Kristallographie - Crystalline Materials* **2005**, *220*, 571. [Crossref]

[26] Dovesi, R.; Orlando, R.; Civalleri, B.; Roetti, C.; Saunders, V. R.; Zicovich-Wilson, C. M. *Z. Cristallogr. - Cryst. Mater.* **2005**, *220*, 571. [Crossref]

[27] Kokalj, A. *Comput. Mater. Sci.* **2003**, *28*, 155. [Crossref]

[28] Paris, E. C.; Espinosa, J. W. M.; de Lazaro, S.; Lima, R. C.; Joya, M. R.; Pizani, P. S.; Leite, E. R.; Souza, A. G.; Varela, J. A.; Longo, E. *Chem. Phys.* **2007**, *335*, 7. [Crossref]

[29] Paris, E. C.; Gurgel, M. F. C.; Joya, M. R.; Casali, G. P.; Paiva-Santos, C. O.; Boschi, T. M.; Pizani, P. S.; Varela, J. A.; Longo, E. *J. Phys. Chem. Solids* **2010**, *71*, 12. [Crossref]

[30] Dudhe, C. M.; Khambadkar, S. J. *J. Alloys Compd.* **2015**, *648*, 92. [Crossref]

[31] Amarande, L.; Miclea, C.; Cioangher, M.; Grecu, M. N.; Pasuk, I.; Negrea, R. F. *J. Eur. Ceram. Soc.* **2014**, *34*, 1191. [Crossref]

[32] Ignácio, C.; Soares, A. R.; Yukimitu, K.; Moraes, J. C. S.; Malmonge, J. A.; Nunes, V. B.; Zanette, S. I.; Araújo, E. B. *Mater. Sci. Eng. A* **2003**, *346*, 223. [Crossref]

[33] Pontes, F. M.; Rangel, J. H. G.; Leite, E. R.; Longo, E.; Varela, J. A.; Araújo, E. B.; Eiras, J. A. *Thin Solid Films.* **2000**, *366*, 232. [Crossref]

[34] Jain, M.; Majumder, S.B.; Guo, R.; Bhalla, A.S.; Katiyar, R. S. *Mater. Lett.* **2002**, *56*, 692. [Crossref]

[35] Pontes, F. M.; Leal, S. H.; Santos, M. R. M. C.; Leite, E. R.; Longo, E.; Soledade, L. E. B.; Chiquito, A. J.; Machado, M. A. C.; Varela, J. A. *Appl. Phys. A: Mater. Sci. Process.* **2005**, *80*, 875. [Crossref]

[36] Verma, K. C.; Kotnala, R. K.; Negi, N. S. *Appl. Phys. A: Mater. Sci. Process.* **2009**, *96*, 1009. [Crossref]

[37] Xie, J.; Hao, H.; Liu, H.; Yao, Z.; Song, Z.; Zhang, L.; Xu, Q.; Dai, J.; Cao, M. *Ceram. Int.* **2016**, *42*, 12796. [Crossref]

[38] Wang, Z.; Cao, M.; Yao, Z.; Li, G.; Song, Z.; Hu, W.; Hao, H.; Liu, H.; Yu, Z. *Ceram. Int.* **2014**, *40*, 929. [Crossref]

[39] Wang, Z.; Cao, M.; Yao, Z.; Song, Z.; Li, G.; Hu, W.; Hao, H.; Liu, H. *Ceram. Int.* **2014**, *40*, 14127. [Crossref]

[40] Xiao, Z.; Zhang, J.; Jin, L.; Xia, Y.; Lei, L.; Wang, H.; Zhang, J.; Xu, S. *J. Alloys Compd.* **2017**, *724*, 139. [Crossref]

[41] Zeng, F.; Cao, M.; Zhang, L.; Liu, M.; Hao, H.; Yao, Z.; Liu, H. *Ceram. Int.* **2017**, *43*, 7710. [Crossref]

[42] Lee, C.; Yang, W.; Parr, R.G. *Phys. Rev. B* **1988**, *37*, 785. [Crossref]

[43] Becke, A. D. *J. Chem. Phys.* **1993**, *98*, 5648. [Crossref]

[44] Nizam, M.; Bouteiller, Y.; Silvi, B.; Pisani, C.; Causa, M.; Dovesi, R. *J. Phys. C: Solid State Phys.* **1988**, *21*, 5351.

[45] Bredow, T.; Heitjans, P.; Wilkening, M. *Phys. Rev. B* **2004**, *70*, 115111. [Crossref]

[46] Corà, F. *Molecular Physics* **2005**, *103*, 2483. [Crossref]

[47] Gatti, C.; Saunders, V. R.; Roetti, C. *J. Chem. Phys.* **1994**, *101*, 10686. [Crossref]

[48] Available from: http://www.tcm.phy.cam.ac.uk/~mdt26/basis_sets/Sr_basis.txt,all%20the%20electron. 09/19/2018.

[49] Xiao, H.; Tahir-Kheli, J.; Goddard, W. A. *J. Phys. Chem. Lett.* **2011**, *2*, 212. [Crossref]

[50] Sambrano, J. R.; Orhan, E.; Gurgel, M. F. C.; Campos, A. B.; Góes, M. S.; Paiva-Santos, C. O.; Varela, J. A.; Longo, E. *Chem. Phys. Lett.* **2005**, *402*, 491. [Crossref]